Clemente Paolo,
ENEA - Casaccia Research Centre
paolo.clemente@enea.it

Giuseppe Delmonaco
Istituto Superiore per la Protezione e la Ricerca Ambientale

Lucamaria Puzzilli
Istituto Superiore per la Protezione e la Ricerca Ambientale

Fernando Saitta
ENEA - Casaccia Research Centre

**Paolo Clemente,
Giuseppe Delmonaco,
Lucamaria Puzzilli,
and Fernando Saitta**

Retrofit Proposal for the Stylite Tower at Umm ar-Raṣāṣ

Abstract

On the basis of the stability and vulnerability analyses carried out on the Stylite Tower at the UNESCO World Heritage Site of Umm ar-Raṣāṣ, Jordan, a proposal for the seismic improvement of the structure is presented in this paper. The main intervention consists in the insertion of a cable or steel bar, connected to a new roof and the existing basement. The reinforcement is tensioned in order to apply a compression axial force on the tower structure. This guarantees a significant increment of the resistant bending moment of the masonry base section. Furthermore, the cable is connected to a central anchor of micro-pile that can guarantee a tension action between the basement and the ground. This would allow for increases to the bending resistance of the interface soil-foundation section.

Introduction

The choice of a suitable intervention on any historic structure should be based on a detailed knowledge of its static and dynamic behavior. Actually, several research studies are reported in the literature for masonry towers, based on both experimental analysis and modelling.

Among the experimental studies, it is worth mentioning the studies carried out on the Cochlid Columns in Rome (Bongiovanni *et al.* 2014; 2017a; 2021), which show the effect of past earthquakes, as well as on the Flaminio Obelisk (Bongiovanni *et al.* 1990), on the Lateran Obelisk (Buffarini *et al.* 2008; 2009), and on the Northern Wall of the Colosseum (Bongiovanni *et al* 2017b). Several experimental studies were also carried out on earthquake damaged towers and constructions (Clemente *et al.* 2002). A comprehensive presentation of the most interesting applications of Structural Health Monitoring in Italy was given by De Stefano *et al.* (2016). Finally, Clemente *et al.* (2015) analyzed the leaning minaret

Studies in the History and Archaeology of Jordan XIV:
Culture in Crisis: Flows of Peoples, Artifacts, and Ideas
Amman: Department of Antiquities, 2022

in Jam, Afghanistan, considering both soil and masonry collapses, under different distributions of static loads along the height, proportionally increasing to the collapse values.

The Stylite Tower at Umm ar-Raṣāṣ, Jordan, is the first known existent and architecturally intact example of this type of tower in the Middle East in this region (DoA 2002). Umm ar-Raṣāṣ has been a UNESCO World Heritage site since 2004. The structure presents damage related to aging and past earthquakes, which frequently affected the area (Sbeinati *et al.* 2005). The damage was first evaluated by means of a comprehensive study of the structure. Then stability and seismic vulnerability analyses were carried out. The results shown here confirm the present precarious condition of the tower and the necessity of urgent and adequate interventions for its structural preservation. Therefore, a retrofitting structural intervention is proposed in this paper. This consists in the insertion of a tensioned reinforcement (a cable or steel bar), connected to a new roof and the existing basement, that applies a compression axial force on the tower structure. Furthermore, the cable is connected to a central anchor of micro-pile that can guarantee a tension action between the basement and the ground. The effects of these interventions are evaluated and discussed.

Stylite Tower and Its Site

The Byzantine Stylite Tower is situated *ca.* 1.2 km NW from the core of the archaeological site of Umm ar-Raṣāṣ, at almost 735 m a.s.l. (Fig. 1). It is well known from historical sources (Brown 1974) that the Christian ascetic monks, called stylites, spent their lives in isolation at the top of a tower, preaching, fasting, and praying.

The geology of the area of Umm ar-Raṣāṣ is characterized by the presence of the al-Ḥasā Phosporite formation (Campanian-Maastrichtian), 55–65 m thick and composed by three different members (Bender 1974; Tarawneh 1985; Powell 1989; Sadaqah *et al.* 2000). The Bahiya coquina member is largely outcropping in the area. This formation, from few meters to 30 m thick, is mostly composed of fossiliferous limestone (rich in oyster shell, foraminifera, gasteropods, and bivalves). A first geotechnical campaign was performed in 2009, with boreholes and laboratory tests on rock materials (Uniaxial Compressive Strength, Point Load tests, rock specific gravity and absorption, chemical analysis; Azzam and Doukh 2009). The blocks of the tower, carved in a quarry close to the Stylite Tower, are of the same material that will be described in detail in section 3.1.

The tower was built in the first half of the 6th c. AD and was originally surrounded by a wall. It is 13.5 m tall and has a square base cross-section with size b = 2.52 m. Externally, the structure presents 35 rows of trimmed local limestone blocks laid dry. Some of the external blocks are placed in order to guarantee a connection with the internal fill.

A small chamber is located at the basement, and remarkably reduces its effective cross-sections (section S2 in Fig. 2). Pilgrims could get into this chamber and communicate with the monk by means of a rectangular hole. This has a 30 × 40 cm size, is eccentrically placed, and continuous for most of its height. Another very small hole was created at the base of the tower for the physiological needs of the monk; its influence on the structural behavior is negligible.

In the lower part of the tower, which can be seen from the base chamber, the fill is made of irregular blocks of similar material forming the tower. In the same lower part of the tower the presence of original mortar among the stones has been detected. The mortar could provide effective bond with the external rows, but the height of the fill and its characteristics are not known as

well as its contribution to the structural capacity.

Some of the stone blocks are cracked, especially those of the base layer whereas other blocks located at different heights show relative displacements. The space between the blocks has recently been filled with stone slabs. The limestone blocks are also affected by different natural exposures and degrees of weathering. Another chamber was originally placed at the top, and that chamber collapsed, along with the dome/vault, probably during a seismic event.

1. The Stylite Tower at Umm ar-Raṣāṣ.

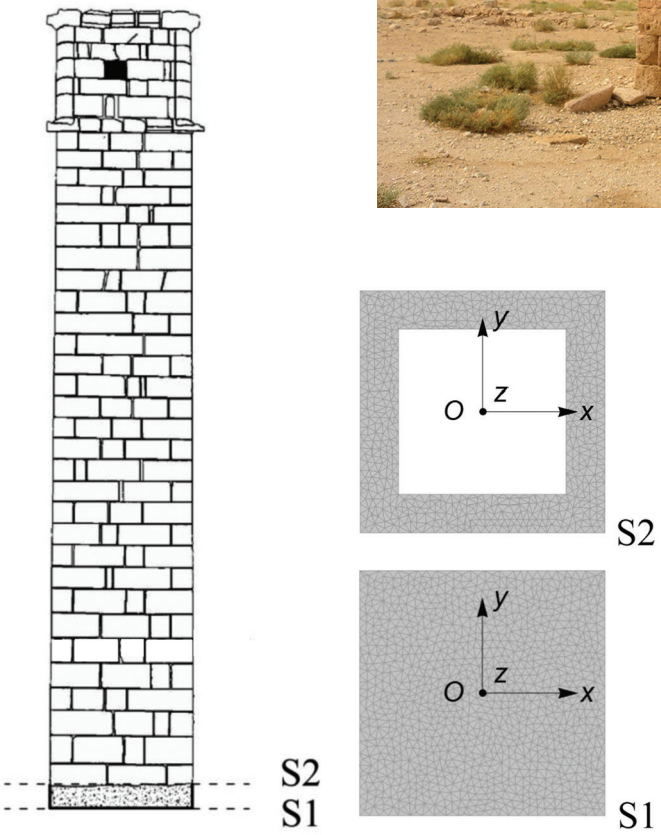

2. Representative cross-sections of the tower.

The foundation is composed of a concrete slab. The slab is the same size as the tower base cross-section, is about 40 cm deep, and placed directedly on the bedrock. Its extrados is at the same level of the ground surface.

A strong earthquake, which occurred in AD 759, caused the collapse of the covering (dome and vaulted roof) and the upper part of the structure. The Jericho earthquake (Ml = 6.2), which occurred on 11 July 1927, is the most recent destructive seismic event that affected the area. This earthquake caused heavy damage in the close cities of as-Salṭ and ʿAmmān and probably also to the Stylite Tower (Avni 1999; Zohar and Marco 2012). The area is characterized by high seismicity with a Peak Ground Acceleration of 0.2 *g* and a shear waves velocity Vs = 760 ÷ 1500 *m/s*, typical of rigid soil (Menahem 1991; Thomas *et al.* 2007).

Previous Studies

A comprehensive experimental campaign was carried out on the tower and the ground in 2014 and 2015 (Clemente *et al.* 2019b). The Uniaxial Compressive Strength (UCS) of the tower's limestone material was assessed *in situ* by means of Schmidt-hammer tests on the stone blocks. Furthermore, 4 passive seismic measurements allowed a field evaluation of the dynamic resonances of the ground. Obviously, destructive mechanical tests on the limestone blocks of the tower were not performed because the Stylite Tower is protected by the Jordanian Antiquity Law.

The results obtained can be summarized as follows:

a) Most of the limestone blocks analyzed, specifically 29 out of 31, showed a medium-high strength (R3 or R4 class) and only very few were in R2 class. These results are consistent with the usual strength value of this material and with UCS values obtained from laboratory analysis for intact limestone blocks of al-Hasā Phosphorite formation (Naghoj *et al.* 2010). It is worth noting that the method used for the evaluation of the strength is based only on the external toughness of the blocks. Actually, the lower values of strength were related to the weathering conditions and the cracks. The latter affect the walls, especially in the NE corner. Anyway, a suitable reduction of the average value obtained experimentally has been considered in the structural analysis.

b) The passive seismic analysis revealed peaks in two ranges of frequency, [1.0, 2.5] Hz and [4.0, 6.0] Hz, respectively. Since the recording sites were very close to the tower, these resonance frequencies were likely induced by the structure and not related to the subsoil (Clemente *et al.* 2019a).

The global stability was also analyzed by referring to the interface section S1 between the ground and the concrete basement slab. The tower was supposed to be infinitely rigid but the section S1 between the ground and the basement was supposed to have an elastic–perfect plastic behavior with a compression strength f_t. On the basis of the experimental analysis of the local limestone described before, a value $f_t \geq 10$ MPa and the corresponding Young's modulus ^{3} 10000 MPa can be supposed (Fener *et al.* 2005; Dweirj *et al.* 2017). These values are also consistent with the characteristics of the concrete basement.

The reference system *Oxyz* with the origin coincident with the center of gravity of the square base cross-section S1, the two axes *x* and *y* parallel to the sides, and the axis *z* vertical can also be assumed. The total weight was estimated as $W = 1800$ kN, including the basement, the fill up to the top, and the covering, once rebuilt. In this hypothesis, the center of gravity is at $z_w = 6.45$ m, while the eccentricity in the plane *xy* is very low; one can assume that the stress point under dead loads only coincides with the center of gravity of the cross-section.

Assuming a model of elastic half space

for the soil, the resulting stability factor was very high (Desideri *et al.* 1997), due to the very high value of the elastic modulus of the soil, apparently ensuring the global stability of the tower.

A push-over seismic analysis was carried out, using a single-model approach. The structure was modelled by means of finite solid elements. Masonry was characterized by an elastic-plastic behavior and a Drucker-Prager limit domain for three-dimensional stress states. 3-D load conditions were considered, using accelerations proportional to the first two modal shapes. Force-displacement capacity curves were obtained by incremental nonlinear static analysis using reasonable values of the cohesion and the friction. The curves show a very low capacity for the tower under seismic actions. Better results were obtained with higher values of the cohesion and with lower values of the friction coefficient, which correspond to more ductile behavior (Clemente *et al.* 2019b).

The Check after Masonry Improvement

The analysis of the tower has been also carried out with reference to the structure after a suitable consolidation. This should consist of the improving of the external masonry, by means of mortar injection or another technique. This external portion of the structure will have higher stiffness and resistance with respect to the internal fill that could be lightened or even partially removed. Therefore, in order to evaluate both situations, two hypotheses were tested: the first considering the fill up to the top, the second with the fill placed only in the lower half of the tower.

In the following paragraph, a simplified model to analyze the nonlinear behavior of section S2 is assumed, in which: a) the fill is considered just for its weight, b) the fill contribution to the structural resistance is neglected, and c) the effective cross-section is a symmetric hollow squared section (Fig. 2). This simplification is justified by the results of a previous analysis in which the effective geometry of S2 was considered.

Then, the model of rigid tower supported by an elastic-plastic cushion that simulates the interaction between the masonry base section and the rigid concrete slab, is analyzed.

Limit Domains of the Base Masonry Cross-Section S2

The model refers to the aforementioned *Oxy* system, with the origin coincident with the center of gravity of the symmetric hollow squared cross-section S2 and the two axes parallel to the sides. The masonry is supposed to have an elastic–perfect

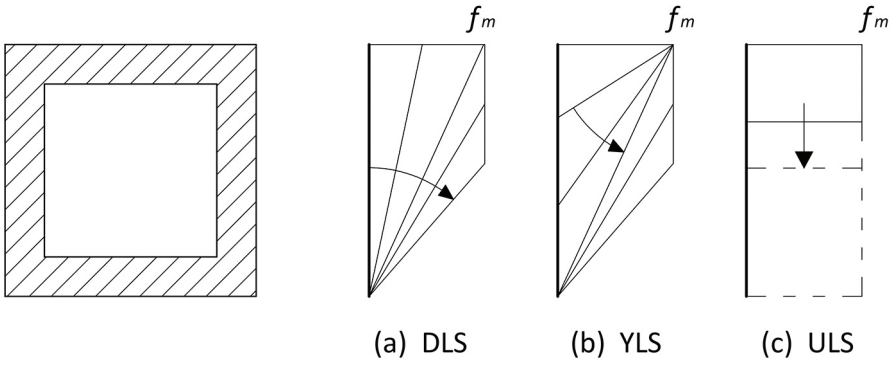

3. Stress distribution in the (a) DLS, (b) YLS, and (c) ULS.

plastic behavior in compression with a strength f_m, but no tension resistance. The effect of an axial load and bending moment around x axis is analyzed. Three limit states must be considered (Fig. 3), corresponding to the decompression, the initial yielding, and the ultimate conditions, respectively. The corresponding limit domains are represented in Fig. 4 in a non-dimensional way, in which:

$$N_0 = 4\,(B-t)\cdot f_m \quad M_0 = \frac{B^3-(B-2t)^3}{8}\cdot f_m \quad (1)$$

are the maximum values of the axial force N and bending moment M, respectively. So the curves are independent of strength f_m. They are also symmetric with respect to N/N_0 axis but for simplicity are plotted only for M > 0.

The cross-section is at its decompression limit state (DLS) if the compression stress is equal to zero at one edge (the lower one in Fig. 3a). The limit domain, in the N/N_0–M/M_0, is characterized by a linear law for $N/N_0 \le 0.5$, corresponding to the case in which the maximum compression stress at the opposite edge $\sigma \le f_m$. For $N/N_0 > 0.5$ the law is nonlinear and corresponds to the cases in which a portion of the cross-section is yielded.

The cross-section is at its initial yielding limit state (YLS) if the compression stress is equal to f_m at one edge (the upper one in Fig. 3b). The limit domain is characterized by a nonlinear law for $N/N_0 \le 0.5$ corresponding to the case in which the cross-section is in a cracked stage (*i.e.*, a portion of the cross-section is not effective and subject to stress equal to zero). For $N/N_0 > 0.5$ the law is linear and corresponds to the cases in which all the section is compressed with the stress varying linearly.

The cross-section is at its ultimate limit state (ULS) if the compression stress is equal to f_m in a portion of the cross-section (the upper one in Fig. 3c) while keeping equal to zero in the other part. The limit domain is characterized by a nonlinear law. When $N/N_0 = 1.0$, the cross-section is uniformly compressed with stress equal to f_m.

The ULS corresponds to a collapse limit state of the cross-section, which is fully yielded in its effective portion. Instead, DLS and YLS correspond to boundaries between different behaviors for the cross-section. It is worth pointing out that when M increases while N keeps constant, DLS occurs first if $N/N_0 \le 0.5$ and the resultant N is at the boundary of the cross-section core. If $N/N_0 < 0.5$ then YLS precedes DLS.

The non-dimensional representation of the limit domains is very useful to analyze the present stress status. This is represented in the diagrams by a point, whose position depends on f_m. It is on the abscissa axis, if the bending moment due to the permanent loads is zero.

The minimum allowable value of f_m is given by the uniform stress under the dead loads, *i.e.*, the ratio between the weight of the tower and the area of S2:

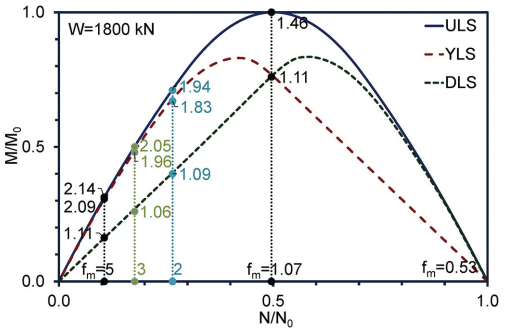

4. Limit domain corresponding to the three limit states and loading paths corresponding to several compression strength of masonry for W = 1800 kN. The labels are the values of the bending moments (MNm).

$$f_{m,\min} = \frac{W}{A} = \frac{1.8}{3.39} = 0.53 \text{ MPa} \qquad (2)$$

If $f_m = 2 \cdot f_{m,min} = 1.07$ MPa, then $N/N_0 = 0.5$.

The limestone blocks are characterized by very dispersed strength values, as pointed out by the experimental analysis. Therefore, a compression strength very close to the lower experimental values was assumed for the stone. Obviously, the strength of a masonry made of these stones is even lower. In the specific case, the absence of the mortar and its bad quality, when present, as well as the irregularity of the joints and the absence of transversal connections or their non-effectiveness must be taken into account. Consequently, the strength is likely in the range 5.0 ÷ 10.0 MPa, and a corresponding Young's modulus between 5000 and 10000 MPa (Naghoj *et al.* 2010). The lower limit values were considered in this study. For $f_m = 5.0$ MPa, it is: $N_0 = 16.96$ MN, $M_0 = 6.82$ MNm and $N/N_0 = W/N_0 = 0.133$.

If the fill will be removed in the upper half portion of the tower, then the total weight will be W = 1500 kN and the stress points will be those in Fig. 5 for the different values of the compression strength f_m.

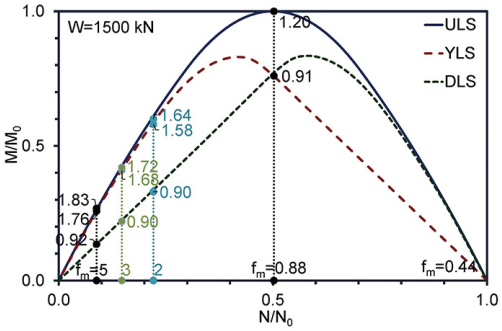

5. Limit domain corresponding to the three limit states and loading paths corresponding to several compression strength of masonry for W = 1500 kN. The labels are the values of the bending moments (MNm).

Nonlinear Analysis

If $N = W$ is fixed and its eccentricity e increases along y, in the plane N/N_0–M/M_0 the loading path is represented by a straight line starting from $(W/N_0, 0)$ and orthogonal to N/N_0 axis. The loading paths relative to different values of f_m are also shown in Fig. 4 for W = 1800 kN and in Fig. 5 for W = 1500 kN. In both cases, the labels reported are the values of the bending moments (MN×m). In Fig. 6 some of the corresponding stress distributions are represented.

The cross-section is entirely effective up to the DLS, when the stress $\sigma = 0$ is at the lower edge (Fig. 6a). From the DLS to YLS the cross-section is in a cracked stage and the stress distribution is still linear with maximum value $\sigma \le f_m$ at the upper edge (Fig. 6b). The relation between the two unknown σ and the depth of the neutral axis ξ is the following:

$$\left[\left(1-\frac{t}{2\xi}\right)(B-2t)+\xi\right] t \cdot \sigma = W \qquad (3)$$

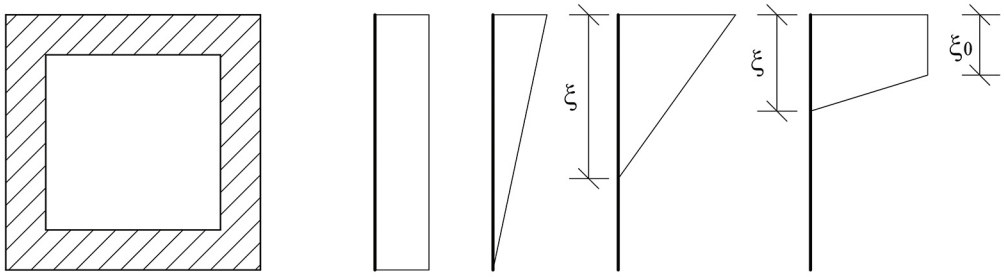

6. Stress distributions corresponding to stress points on the loading path.

From eq. (3), for any value of ξ the corresponding value of σ can be deduced.

From YLS to ULS the stress law is divided into two portions (Fig. 6c): it is constant and equal to f_m for a depth ξ_0 from the upper edge and then decreases linearly to the neutral axis at ξ. In this case, the relation between the two unknowns ξ and ξ_0 is:

$$\frac{Bf_m}{2} \cdot (\xi_0 + \xi) = W \tag{4}$$

If the increment of the bending moment *M* is related to a horizontal seismic acceleration *a(z)* acting in *y* direction, then the resultant force is:

$$F = \int_0^H m(z) \cdot a(z) \cdot z dz \tag{5}$$

It is applied at the height:

$$z_F = \frac{\int_0^H m(z) \cdot a(z) \cdot z dz}{\int_0^H m(z) \cdot a(z) \cdot dz} \tag{6}$$

It is $z_F = 2H/3$ in the hypothesis of mass constant along the height.

From the equilibrium condition one can deduce the relation between *F/W* and the rotation α at the base (where the eccentricity *e* is a function of the rotation α):

$$F = \frac{1}{z_F} (e - z_w \cdot a) \tag{7}$$

The generalized displacement *d* is deduced as ratio between the work *L* of the external load and the force *F*:

$$D = \frac{L}{F} = \frac{\int_0^H m(z) \cdot a(z) \cdot d(z) \cdot dz}{\int_0^H m(z) \cdot a(z) \cdot dz} \tag{8}$$

Retrofit Intervention

The proposed intervention consists of:

a) improvement of the external masonry, in order reach at least the considered value f_m = 5.0MPa
b) reconstruction of the covering structure in steel or wood
c) insertion of a cable or steel element to apply compression in the tower, without adding mass
d) foundation anchor or pile to anchor the cable or steel element to the soil and so the tower

Alternatively, a new sub-foundation could be built, wider than the existing one, connected to it and composed of 4 micro-piles at its corners. Furthermore, the hypothesis of reduction of the fill was also considered.

Masonry Improving

Points a) and b) will determine the final weight of the tower, which should be not much higher than the present one, and new stress points with the associated loading path. The already described non-dimensional domains are still valid.

Point c) consists of the insertion of a cable or steel element (Fig. 7). The cable will be fixed to a new roof at the top of the tower and the concrete basement, and then pre-tensioned. With reference to the case of f_m = 5.0MPa, increases of the axial force by 1.5 and 2.0 were considered.

In Fig. 8, the corresponding loading paths due to an increase of the bending moment are plotted. The values reported as labels at the intersection points with the limit domains, are the ratios between the bending moment at each point and the corresponding one obtained for N = W. These are exactly equal to the increase of the axial force up to the DLS, but are lower for the other limit states. Anyway, the efficiency of the intervention is apparent.

Analogously, the stress points and the corresponding loading paths for W = 1500 kN are plotted in Fig. 9. The increments of

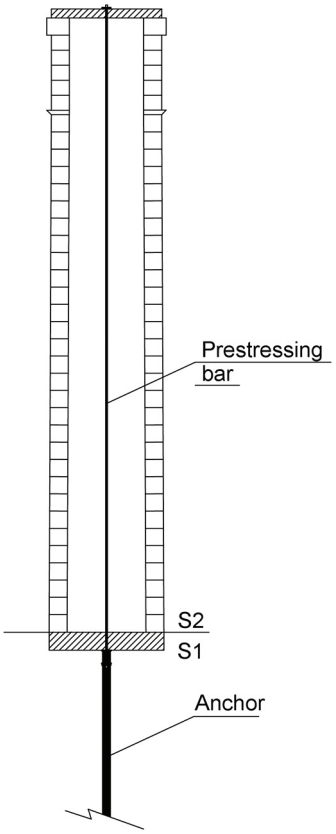

7. Retrofitting intervention with a single central anchor element.

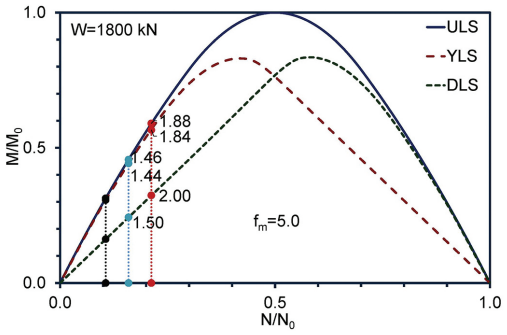

8. Limit domain corresponding to the three limit states and loading paths corresponding to difference axial forces N = W = 1800 kN, N = 1.5 W, N = 2.0 W (f_m = 5.0 MPa). The labels are the ratios between the bending moments and those for N = W.

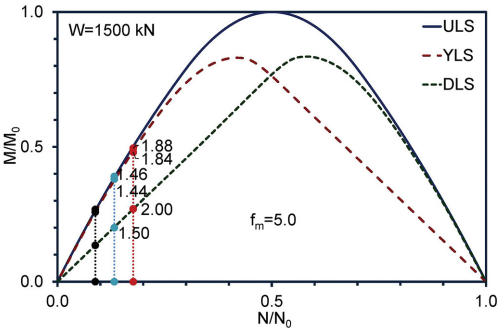

9. Limit domain corresponding to the three limit states and loading paths corresponding to difference axial forces N = W = 1500 kN, N = 1.5 W, N = 2.0 W (f_m = 5.0 MPa). The labels are the ratios between the bending moments and those for N = W.

the bending moment, reported as labels, are obviously independent of the total weight W of the tower.

Foundation Improving

Point d) consists of the insertion of a central anchor or micro-pile, built along the same straight line of the cable, which will anchor the tower to the ground (Fig. 7). The anchor will be not active, but put in action only under a bending moment that determines traction at the base interface between the tower and the ground.

In Fig. 10 the limit domains of the squared base section S1 are plotted. For example, the stress points relative to f_m = 5.0 are considered. Furthermore, the stress point relative to a seismic acceleration equal to 0.3 *g* is plotted.

If completely yielded, the anchor introduces an axial force but no bending moment with reference to the gravity center of the cross-section S1. Therefore, the limit domain translates to the left

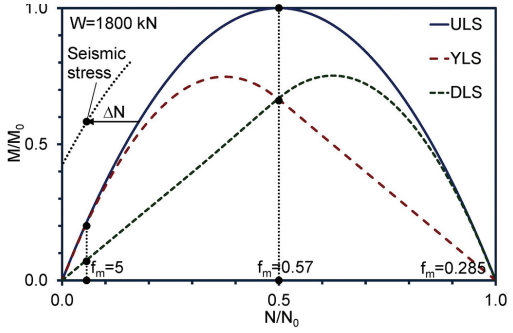

10. Limit domain corresponding to the three limit states of S1, with loading path for f_m = 5.0 MPa for W = 1800 kN; seismic stress point and translated domain (dotted line).

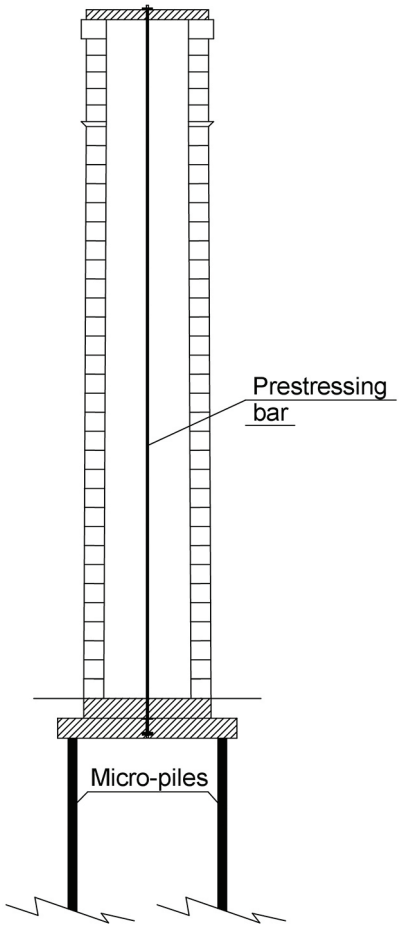

11. Retrofitting intervention with a sub foundation with four micro-piles.

side. The horizontal distance between the limit domain of the cross-section without anchor and the seismic stress point gives the characteristics of the anchor element (Raithel 1982).

Obviously, an anchor element with a certain eccentricity will be more effective, although in this case at least 4 anchor elements (preferably micro-piles) will be necessary (Fig. 11).

Conclusions

Starting from previous studies carried out by the authors on the stability and seismic vulnerability of the Stylite Tower at Umm ar-Raṣāṣ, a possible retrofitting intervention for the tower has been presented in this paper. The intervention consists of the insertion of a pre-tensioned cable or steel bar, connected to a new roof at the top and to the existing basement, in order to apply a compression axial force on the tower structure. Furthermore, the cable will be connected to a central anchor of micro-pile that can guarantee a tension action between the basement and the ground.

The preliminary analysis has demonstrated that an increment of the axial force of 50 or 100% will significantly increase the resistant bending moment of the masonry base section S2. The limit analysis of the section S1 revealed the limited resistance to bending moments in its present configuration. A preliminary evaluation of the needed strength of the central anchor of micro-pile has also been done.

Acknowledgements

The present study contributes to meeting the requirements set by the UNESCO World Heritage Center addressed to the Department of Antiquities of the Hashemite Kingdom of Jordan (DoA) for the conservation of the Stylite Tower of Umm ar-Raṣāṣ. It is part of a collaboration between the DoA, ISPRA, and ENEA. The authors are grateful to Mr. Yazid Elayan

(Director General, DoA), Prof. Monther Jamhawi (former Director General, DoA), and DoA staff for their continuous support and encouragement for the studies conducted.

Bibliography

Avni, R. 1999. "The 1927 Jericho Earthquake. Comprehensive Macroseismic Analysis Based on Contemporary Sources." Ph.D. diss, Ben Gurion University of the Negev, Beer Sheva (in Hebrew).

Azzam, M., and F. Doukh. 2009. *Site Investigation for Saint Stylite Tower at Um er-Rasas/Madaba. Annex 1: Geological Report for the Stylite Tower*. Amman: Technical Report, Natural Resources Authority.

Bender, F. 1974. *Geology of Jordan*. Berlin: Gebruedre.

Bongiovanni, G., G. Buffarini, P. Clemente, D. Rinaldis, and F. Saitta. 2017a. "Experimental Vibration Analyses of a Historic Tower Structure." *Journal of Civil Structural Health Monitoring* 7:601–13. doi: 10.1007/s13349-017-0245-4.

———. 2017b. "Dynamic Characteristics of the Amphitheatrum Flavium Northern Wall from Traffic-Induced Vibrations." *Annals of Geophysics* 60:S0439. doi: 10.4401/ag-7178.

Bongiovanni, G., G. Buffarini, P. Clemente, and F. Saitta. 2014. "Ambient Vibrational Analysis of Aurelian Column." *Proceedings of the 10th U.S. National Conference on Earthquake Engineering (10NCEE, Anchorage, AK, 21–25 July)*. Paper 1013, EERI. doi: 10.4231.D35717P1T.

———. 2021. "Time and Frequency Domain Analyses in the Experimental Dynamic Behaviour of the Marcus Aurelius' Column." *International Journal of Architectural Heritage* 15:64–78. doi: 10.1080/15583058.2019.1706785.

Bongiovanni, G., M. Celebi, and P. Clemente. 1990. "The Flaminio Obelisk in Rome: Vibrational Characteristics as Part of Preservation Efforts." *Earthquake Engineering and Structural Dynamics* 19:107–18. doi: 10.1002/eqe.4290190110.

Brown, P. 1971. "The Rise and Function of the Holy Man in Late Antiquity." *JRS* 61:80–101.

Buffarini, G., P. Clemente, A. Paciello, and D. Rinaldis. 2008. "Vibration Analysis of the Lateran Obelisk." *Proceedings of* 14th World Conference on Earthquake Engineering (14WCEE, Beijing, 12–17 October). Paper S11-055. St. Louis: IAEE & CAEE, Mira Digital Publishing.

———. 2009. "The Lateran Obelisk: Experimental Analysis and Modelling." In *Protection of Historical Buildings, PROHITECH 09 (Proceedings of International Conferece on Protection of Historical Buildings, Rome, Italy, 21–24 June)*. Vol. 1, edited by F.M. Mazzolani, 841–8. London: Taylor & Francis Group.

Clemente, P., G. Bongiovanni, and G. Buffarini. 2002. "Experimental Analysis of the Seismic Behaviour of a Cracked Masonry Structure." *Proceedings of 12th European Conference on Earthquake Engineering (London, 9–13 September)*. Paper No. 104. London: Elsevier Science.

Clemente, P., G. Delmonaco, L. Puzzilli, and F. Saitta. 2019a. "Seismic Analysis of the Stylite Tower at Umm ar-Rasas." In *Structural Analysis of Historical Constructions. RILEM Bookseries* 18, edited by R. Aguilar, D. Torrealva, S. Moreira, M.A. Pando, and L.F. Ramos, 1780–7. Cham: Springer. doi: 10.1007/978-3-319-99441-3_191.

———. 2019b. "Stability and Seismic Vulnerability of the Stylite Tower at Umm ar-Rasas." *Annals of Geophysics* 62:SE340, INGV. doi: 10.4401/ag-8004.

Clemente, P., F. Saitta, Buffarini, and L. Platania. 2015. "Stability and Seismic Analyses of Leaning Towers: The Case

of the Minaret in Jam." *The Structural Design of Tall and Special Buildings* 24:4058. doi: 10.1002/tal.1153.

De Stefano, A., E. Matta, and P. Clemente. 2016. "Structural Health Monitoring of Historical Heritage in Italy: Some Relevant Experiences." *Journal of Civil Structural Health Monitoring* 6:83–106. doi: 10.1007/s13349-016-0154-y.

Desideri, A., G. Russo, and C. Viggiani. 1997. "The Stability of Towers on Deformable Ground." *Rivista Italiana di Geotecnica* 1:21–9.

DOA. 2002. *The Old City of Umm ar-Rasas (Mefa'a), Nomination File Submitted to the World Heritage Bureau and Committee for Inscription on the World Heritage List, Amman*. Amman: Department of Antiquities of the Hashemite Kingdom of Jordan.

Dweirj, M., F. Fraige, H. Alnawafleh, and A. Titi. 2017. "Geotechnical Characterization of Jordanian Limestone." *Geomaterials* 7:1–12.

Fener, M., S. Kahraman, A. Bilgil, and O. Gunaydin. 2005. "A Comparative Evaluation of Indirect Methods to Estimate the Compressive Strength of Rocks." *Rock Mechanics and Rock Engineering* 38:329–43.

Menahem, A.B. 1991. "Four Thousand Years of Seismicity Along the Dead Sea Rift." *Journal of Geophysical Research* 96(B12):20195–216.

Naghoj, N.M., N.A.R. Youssef, and O.N. Maaitah. 2010. "Mechanical Properties of Natural Building Stone: Jordanian Building Limestone as an Example." *Jordan Journal of Earth and Environmental Sciences* 3:37–48.

Powell, J.H. 1989. *Stratigraphy and Sedimentation of the Phanerozoic Rocks in Central and South Jordan.* Amman: Natural Resources Authority, Geological Mapping Division.

Raithel, A. 1982. *Metodo semiprobabilistico agli stati limite*. Naples: Liguori Editore.

Sadaqah, R.M. 2000. "Phosphogenesis, Geochemistry, Stable Isotopes and Depositional Sequences of the Upper Cretaceous Phosphorite Formation in Jordan." Ph.D. diss., University of Jordan.

Sbeinati, M.R., R. Darawcheh, and M. Mouty. 2005. "The Historical Earthquakes of Syria: An Analysis of Large and Moderate Earthquakes from 1365 BC to 1900 AD." *Annals of Geophysics* 48:347–435.

Tarawneh, B. 1985. *The Geology of Al-Hisa (Al I'na). Map Sheet No. 3151-I*. Amman: Natural Resources Authority.

Thomas, R., T.M. Niemi, and S.T. Parker. 2007. "Structural Damage from Earthquakes in the Second-Ninth Centuries at the Archaeological Site of Aila in Aqaba, Jordan." *BASOR* 346:59–77.

Zohar, M., and S. Marco. 2012. "Re-estimating the Epicenter of the 1927 Jericho Earthquake Using Spatial Distribution of Intensity Data." *Journal of Applied Geophysics* 82:19–29.